Laser photothermal diagnostics of genuine and counterfeit British and United States banknotes

Andreas Othonos
Andreas Mandelis,* MEMBER SPIE
Marios Nestoros
Constantinos Christofides
University of Cyprus
Faculty of Pure and Applied Sciences
Department of Natural Sciences
P.O. Box 537
CY-1678 Nicosia, Cyprus
E-mail: mandelis@me.utoronto.ca

Abstract. Laser-induced, frequency-scanned IR photothermal radiometry was used to investigate the thermophysical properties of the paper on which several genuine and counterfeit British (£10) and U.S. ($50, $100) currency bills were printed. The radiometric photothermal amplitudes and phases were further compared with a theoretical model, which yielded simultaneous quantitative measurements of the thermal diffusivities and conductivities of the bills. Both statistical and single-specimen results demonstrated the excellent thermophysical resolution of the technique with prospects for its use in the nonintrusive, on-line identification of counterfeit banknotes.

Subject terms: photoacoustic and photothermal science and engineering; infrared; radiometry; photothermal; diagnostics; banknotes.

Paper PPS-08 received May 15, 1996; accepted for publication June 24, 1996.

1 Introduction

Laser-induced IR photothermal radiometry (PTR) has been established as a nondestructive evaluation technique for many classes of solid materials.[1,2] This technique relies on the monitoring of modulated thermal (blackbody) radiation emitted from an optically excited surface of a material after photothermal excitation by a laser. Following partial or total absorption of the incident radiation, a portion of it is converted into heat.[3] Generally speaking, a major advantage of photothermal techniques over purely optical methods is their ability to frequently yield reliable measurements of the thermophysical properties of condensed phases of, for instance, efficient light scattering materials, which do not allow their characterization through conventional optical means.[4] Very recently,[5] PTR was applied successfully and for the first time to the measurement of the thermophysical properties of commercial xerographic paper sheets, on which neither conventional modulated optical transmission nor Fourier transform IR (FTIR) spectroscopy could be performed, owing to the very high density of optical scattering centers in paper. Nevertheless, on the application of PTR, laser-intensity modulation frequency scans were performed and high-quality, very stable and reproducible radiometric signals were obtained. A 1-D theoretical model of the photothermal signal was subsequently developed and compared with the experimental data.[5] As a result, the thermal diffusivity and thermal conductivity of the paper samples were calculated.

An extension of the foregoing investigation to the forensic domain is timely and is the object of this paper. Our theoretical simulations and experimental findings in Ref. 5 indicated that reliable measurements of the thermophysical properties of paper may be made, based on simple best-fitting procedures of the theory to the data, taking into account the optical constants of a thin printed surface layer and those of the bulk substrate paper. These constants are the effective optical absorption and scattering coefficients of the paper at the laser excitation wavelength, and those within the IR emission bandwidth of the IR blackbody detector. The particular features of the experience gained from laser PTR paper product investigations of potential value to forensic identification of counterfeit currency bills are (1) the relative insensitivity of the frequency-scanned profile of the transmission radiometric signal to the condition and/or the color of the surface of the paper and (2) the high sensitivity of the signal to the bulk (substrate paper) thermal diffusivity and, to a lesser extent, to bulk thermal conductivity.

Therefore, this technique is, in principle, capable of identifying currency forgeries based on the nature and texture of the paper matter on which the particular currency dye has been deposited and printed. In current police practice, counterfeit bill identification and analysis methodologies are entirely surface oriented.[6] They include simple optical-microscope and visual examinations of suspect bills with a ''trained eye'' through a magnifying lens, with emphasis on discrepancies in specific feature reproductions (which are becoming increasingly highly sophisticated in major world currency counterfeit bills), or on variations in the chemistry of the surface dye layer itself.

In this paper, experimental laser PTR results from selected genuine and counterfeit British and American banknotes are presented and compared with theoretical predictions from a 1-D theoretical model of the PTR signal. The existence of the model[5] enabled the calculation of thermal diffusivities and conductivities and statistical or one-to-one comparisons between the genuine and the counterfeit samples.

*On leave from: University of Toronto, Photothermal and Optoelectronic Diagnostics Laboratories (PODL), Toronto M5S 3G8, Canada.

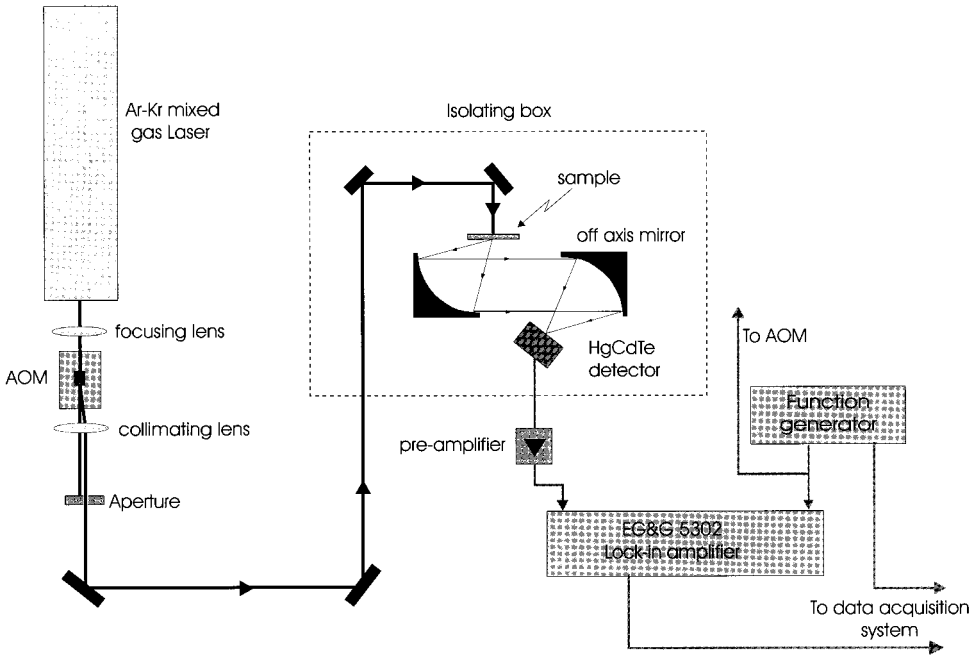

Fig. 1 Experimental setup for frequency-scanned transmission PTR: AOM, acousto-optic modulator; MCT: EG&G Judson J15-D12 HgCdTe detector fitted with a Ge window.

2 Methodology and Results

Figure 1 shows the PTR experimental setup used to perform frequency scans of selected currency bills: a continuous-wave (cw) Ar-Kr laser from Coherent (Innova 70) emitting at mixed 488 and 514.5 nm was used as an unfocused pump beam of spot size ~4 mm, with output power on the order of 100 mW. The intensity of the laser was harmonically modulated using an external sine-wave generator to drive the acousto-optic modulator and to change automatically the modulation frequency applied to it. The frequency scan was in the range 2 to 1000 Hz, consistent with predetermined thermal energy transport rates across the banknotes studied in this work. Two Ag-coated off-axis paraboloidal mirrors were used to capture and collimate the IR radiation and, subsequently, to focus it on the active area of a liquid-nitrogen-cooled mercury-cadmium-telluride (MCT:HgCdTe) detector/preamplifier circuit with frequency bandwidth between dc and 1 MHz. The detector was fitted with a Ge window, which filtered out the excitation beam. The spectral response of the detector was in the 2 to 12 μm range. The PTR signal from the preamplifier (EG&G Judson Model PA-350) was fed into the lock-in analyzer (EG&G Model 5302). This setup enabled computer-controlled, automatic frequency scans of the acousto-optically modulated laser intensity. The amplitudes and phases of the PTR signals were stored in the computer for theoretical analysis and calculations. Normalized amplitude and phase curves were further obtained by dividing the former by the respective signal amplitude of, and subtracting from the latter the respective signal phase from, a thick (''semi-infinite'') piece of steel acting as a reference sample. When the spot-size of the laser beam is large compared to the thermal diffusion length

$$\mu_s(\omega)=\left(\frac{2\alpha_s}{\omega}\right)^{1/2}, \tag{1}$$

where ω is the angular modulation frequency of the laser beam intensity, and α_s is the thermal diffusivity of the sample, then a 1-D thermal wave is launched in the bulk of the sample with very simple frequency dependence[7]:

$$|S_T|\propto\omega^{-1/2} \tag{2}$$

and

$$\Phi_T\propto-\frac{\pi}{4}=\text{const.} \tag{3}$$

Therefore, when the *experimental* amplitude from a currency bill is divided by that of the reference sample, which may contain experimental-system-related frequency dependencies, for comparison with theory, the *theoretical* amplitude must also be normalized through multiplication by $\sqrt{\omega}$, which assumes flat instrumental frequency response. Similarly, when $\pi/4$ is added to the *theoretical* phase, the phase should be directly comparable to the normalized *experimental* phase, which is obtained by subtraction of the reference sample phase.

Genuine and counterfeit bills representing two major world currencies, namely British £10 and U.S. $50 and $100 denominations, all of measured thicknesses 82.5 ± 2.0 μm, were used in our investigations for optical transmission, FTIR and laser PTR experiments. For the optical transmission tests the acousto-optically modulated Ar-Kr laser beam was incident normal to the surface of the sample and a sensitive photodiode was placed on the other

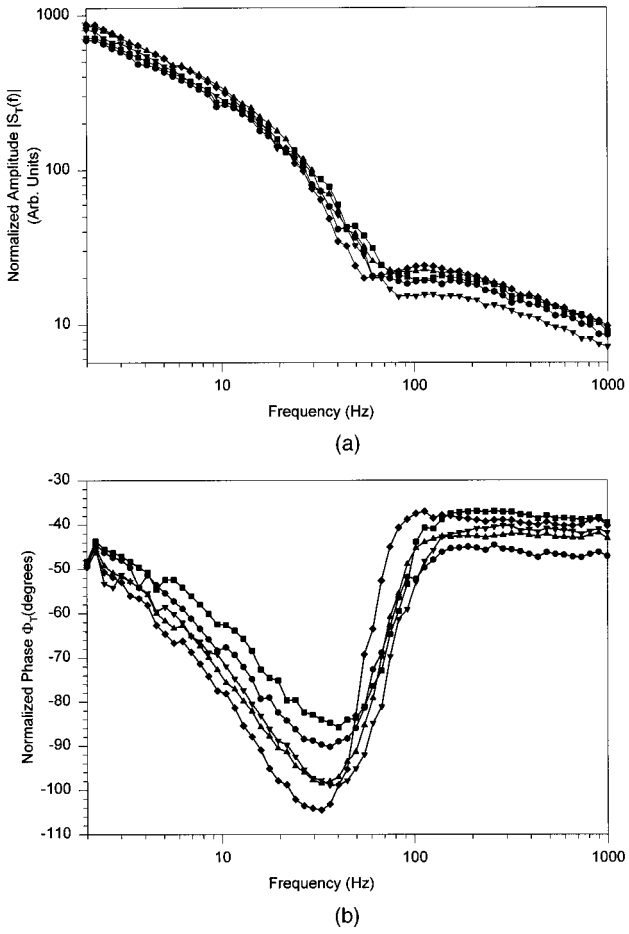

Fig. 2 (a) Normalized experimental PTR amplitudes and (b) normalized phases of the frequency responses of four genuine and one counterfeit British £10 bills of thicknesses 82±2 μm: diamonds, counterfeit sample.

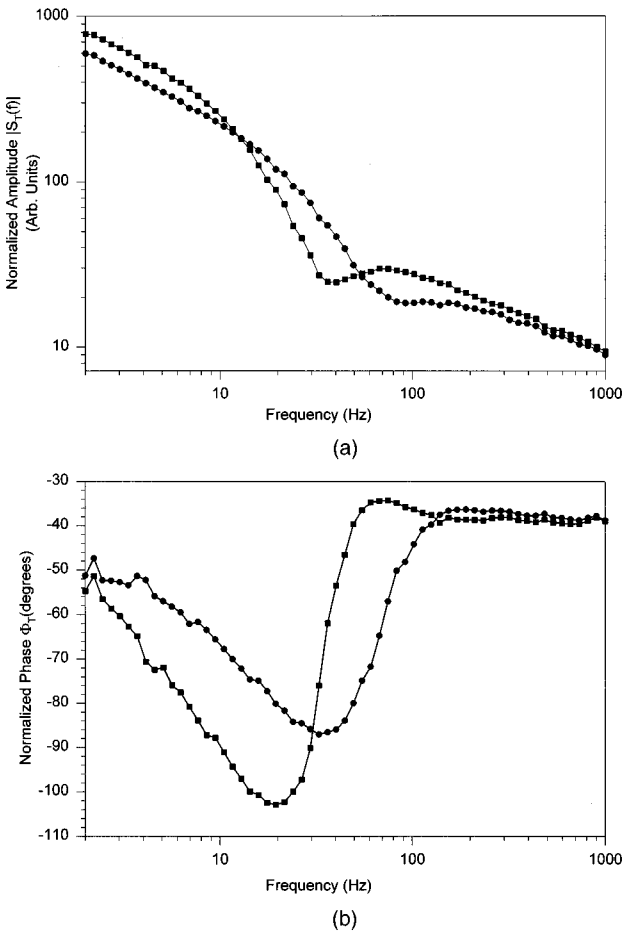

Fig. 3 (a) Normalized PTR experimental amplitude and (b) normalized phase of the frequency response of one genuine (dots) and one counterfeit (squares) U.S. $50 bill of thicknesses 82±2 μm.

side. As expected,[5] no signal could be detected, owing to the large scatter of the light across the body of the bills. Similarly negative results were obtained from the FTIR transmission and back-scattering experiments. The samples were subsequently fixed on the sample holder of the laser PTR instrument of Fig. 1 with removable adhesive tape, the laser was defocused, and its power was adjusted so as to be well below the optical damage threshold of the paper. The laser-generated ac PTR signals, unlike their purely optical counterparts, were stable and reproducible. Frequency scans were performed with a group of four genuine £10 bills to obtain acceptably meaningful statistical fluctuations of the thermophysical parameter values of the genuine currency. Only one genuine $50 and $100 bills were tested. One counterfeit bill of highly accurate visual reproduction and convincing quality of texture was available for each of the foregoing denominations. The PTR amplitude and phase responses from the £10 bills are shown in Fig. 2. Figure 3 shows similar results obtained from the $50 bills. Figure 4 shows the results obtained from the $100 bills.

3 Theoretical Interpretation of the Data and Discussion

A 1-D model of the PTR signal from paper with a surface absorbing layer has been presented in Ref. 5 and is schematically shown in Fig. 5. In summary, the infrared photothermal radiometric signal from the free-standing sheet of paper (or a banknote) is given by

$$S_T(\omega)=K\beta_{\mathrm{IR}}\left\{C_1\left[\frac{\exp(-\sigma_s L)}{\beta_{\mathrm{IR}}-\sigma_s}\right]+C_2\left(\frac{e^{\sigma_s L}}{\beta_{\mathrm{IR}}+\sigma_s}\right)-\left(\frac{C_1}{\beta_{\mathrm{IR}}-\sigma_s}+\frac{C_2}{\beta_{\mathrm{IR}}+\sigma_s}\right)\exp(-\beta_{\mathrm{IR}}L)-A\left[\frac{\exp(-\beta_s L)-\exp(-\beta_{\mathrm{IR}}L)}{\beta_{\mathrm{IR}}-\beta_s}\right]\right\} \tag{4}$$

where the constants $C_1(\omega)$ and $C_2(\omega)$ are defined as follows:

$$C_1=\frac{1}{[(1+b_{gs})^2e^{\sigma_s L}-(1-b_{gs})^2\exp(-\sigma_s L)]}\times\left\{A[(1-b_{gs})(b_{gs}-r_s)\exp(-\beta_s L)+(1+b_{gs})\times(b_{gs}+r_s)e^{\sigma_s L}]+\frac{I_o(1+b_{gs})(1-e^{-Q})}{2k_s\sigma_s}e^{\sigma_s L}\right\} \tag{5}$$

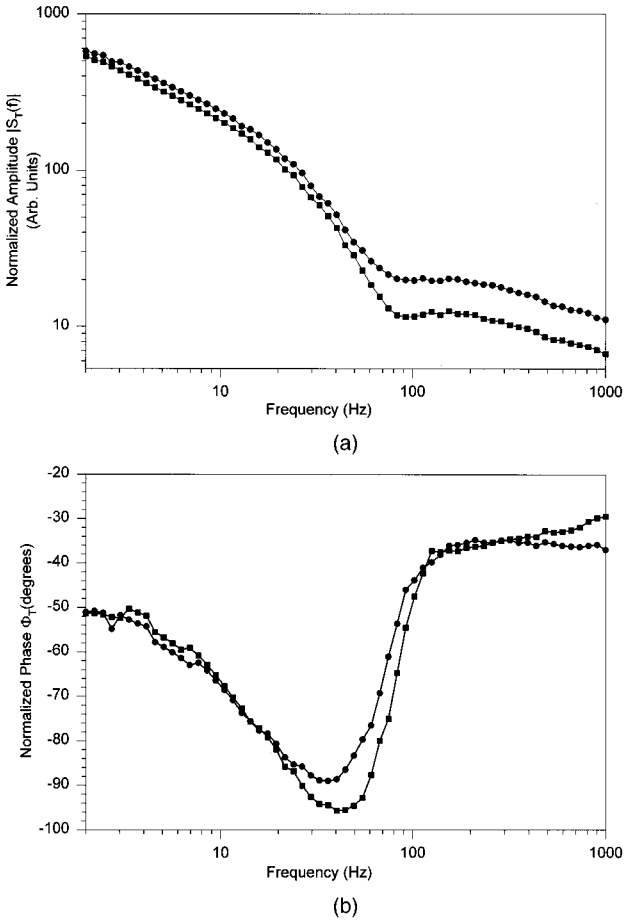

Fig. 4 Similar to Fig. 3 for a genuine (dots) and a counterfeit (squares) U.S. $100 bill.

and

$$C_2=\frac{1}{[(1+b_{gs})^2e^{\sigma_sL}-(1-b_{gs})^2\exp(-\sigma_sL)]}\times\left\{A[(1+b_{gs})(b_{gs}-r_s)\exp(-\beta_sL)+(1-b_{gs})\times(b_{gs}+r_s)\exp(e^{-\sigma_sL})]+\frac{I_o(1-b_{gs})(1-e^{-Q})}{2k_s\sigma_s}\times\exp(-\sigma_sL)\right\}. \quad (6)$$

In Eqs. (4) to (6) the following definitions were made:

$$A(\omega)=\frac{I_o\beta_s}{2k_s(\beta_s^2-\sigma_s^2)}e^{-Q} \quad (7)$$

and

$$b_{gs}\equiv\frac{k_g\sqrt{\alpha_s}}{k_s\sqrt{\alpha_g}}\ ;\ r_s\equiv\frac{\beta_s}{\sigma_s}, \quad (8)$$

where

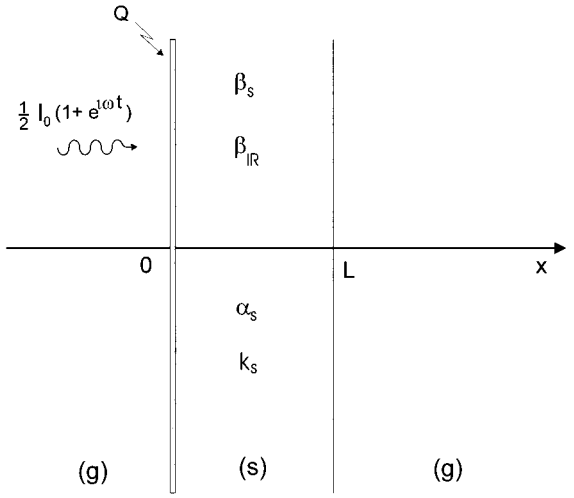

Fig. 5 Schematic of 1-D geometry for transmission IR photothermal radiometry of banknotes: (g), gas (air); and (s), solid layer of thickness L, thermal diffusivity α_s, thermal conductivity k_s, and effective optical absorption coefficient β_s (visible) and β_{IR} (IR). The incident visible-range laser radiation has intensity I_o and angular modulation frequency $\omega=2\pi f$. The surface of the specimen is assumed to have a thin uniform dye layer of absorbance Q (= surface absorption coefficient × effective layer thickness).

$$\sigma_j=(1+i)\left(\frac{\omega}{2\alpha_j}\right)^{1/2}\quad j=g(\text{gas;air}),\quad s(\text{sample}). \quad (9)$$

The physical meaning of the various symbols appearing in Eqs. (4) to (9) is given in the caption of Fig. 5. The optical constants β_s and β_{IR}, although defined in the theory as *optical absorption coefficients*, must be taken as combined *absorption and scattering coefficients*, where it will be tacitly assumed that their values are homogeneous throughout the bulk of the paper.

Initial visual examination of the raw data curves from the various samples in Fig. 2 reveals that there are definite differences both within the group of genuine £10 bills and, more importantly, between this group and the counterfeit sample. The most notable features are the local minima in the amplitude and phase data, as well as the steep phase increase past the minimum to its eventual leveling-off in the range >100 Hz. The position of the amplitude minimum of the counterfeit bill lies well to the left of those within the statistical group of the four genuine bill amplitudes. A similar trend is evident with the (much broader) phase minima. More significantly, the position of the rising edge of the counterfeit phase in the frequency range 40 Hz$<f<$100 Hz, behaves very differently from the group of four, which enhances the diagnostic resolution capability of PTR in this case. Strong differences between the amplitudes and especially the phases of the $50 bills are shown in Fig. 3. These differences occur across the modulation frequency spectrum and may constitute a definitive diagnostic of the falsity of the counterfeit in cases such as this one, where the visual and textural quality of the bill was such that, very likely, the forgery would pass unnoticed by anyone other than trained forensic professionals. Unfortunately, in this first forensic investigation/evaluation of laser PTR there were no more U.S. $50 available in our labora-

Table 1 Thermophysical properties of selected currency denomination and their counterfeits.

Genuine Denomination	Counterfeit Denomination	Thermal Diffusivity ($\times 10^{-8}$ m^2/s)	Thermal Conductivity ($\times 10^{-4}$ W/mK)
£10 (#1)		5.2	9.4
£10 (#2)		6.2	13.0
£10 (#3)		5.0	10.0
£10 (#4)		5.3	11.0
£10 (averaged)		5.43±0.27	10.85±0.39
	£10	3.2	4.0
$50		5.4	11.0
	$50	2.2	3.0
$100		5.4	10.0
	$100	6.2	13.0

tory to perform a study on the statistical variations within a group of genuine bills. A similar situation existed with the $100 bills. In this case, however, Fig. 4 shows that the counterfeit sample was made of paper with thermophysical properties much closer to the genuine bill than the $50 forgery. Notice that the degree of dissimilarity between the genuine and counterfeit increases with increased frequency for both amplitude and phase, with the greatest variations to be found in the range $f > 80$ Hz (amplitude) and $f > 20$ Hz (phase).

Subsequently, theoretical curves superposed on the data pairs (amplitude and phase) of Figs. 2 to 4 were obtained following a trial-and-error procedure for optimally fitting Eq. (4). It can be seen from Eq. (4) that the fit is a multivariable one involving five parameters: α_s, k_s, β_s, Q, and β_{IR}. Unfortunately, no independent measurements of, at least, the optical parameters were available, as all our optical experiments were inconclusive; therefore, the simultaneous variation of all five parameters toward a best fit raises the issue of the uniqueness of the fit. Even though there can be no rigorous proof of the uniqueness of the calculated best-fit set of parameters, the requirement for the theory to yield acceptable fits to both amplitude and phase data proved to yield stringent enough constraints, so as to raise the level of confidence in how meaningful (or even unique) the sets of calculated parameters were. Furthermore, it was observed earlier[5] that the values of the various parameters in the curve-fitting procedure affected the nature and shape of the curves differently, with the result that the thermophysical parameter value ranges could be effectively isolated and determined separately from those of the optical parameters. This important observation, plus the much higher degree of sensitivity of the theoretical curves to the value of thermal diffusivity than to thermal conductivity, were convincing empirical evidence of the uniqueness of our fits. In any case, the value of the present noncontact technique is expected to lie more in its comparative diagnostic capabilities among relative rather than absolute sets of data, and may be quite adequate for on-line use with minimal data analysis, on construction of the appropriate calibration curves for each denomination of a given currency.

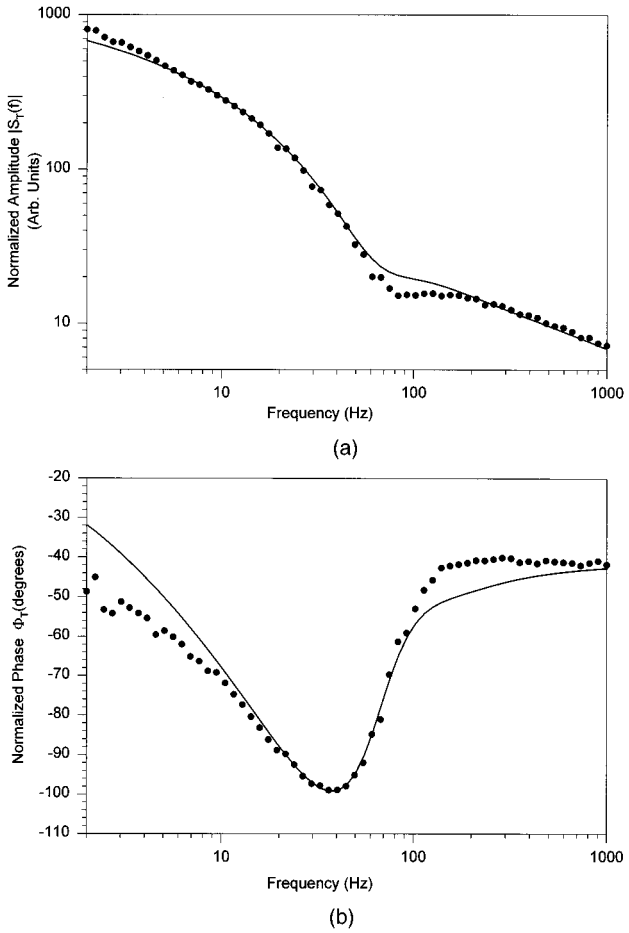

Fig. 6 (a) Normalized amplitude and (b) normalized phase of the frequency response of a genuine British £10 bill: dots, experimental data; solid line, simultaneous theoretical best fits to the amplitude and phase of Eq. (4). For the best-fit thermophysical parameters see Table 1. The optical parameters were $\beta_s = 5.7 \times 10^4$ m^{-1}, $\beta_{\mathrm{IR}} = 7.7 \times 10^4$ m^{-1}, and $Q = 0.7$.

For the calculation of the thermal coupling coefficient b_{gs} the literature values[8] for air were used: $k_g = 2.38 \times 10^{-2}$ W/mK and $\alpha_g = 2 \times 10^{-5}$ m^2/s. For simplicity and speed, the normalized theoretical [see Eqs. (2) and (3)] and experimental curves were matched arbitrarily at one frequency, and then optimal theoretical fits of the amplitude and phase of Eq. (4) to the rest of each data set were made. When independent theoretical fits to either the amplitude or phase of the PTR signal were attempted, several widely different sets of the parameters could be found, each giving excellent fits to the data. Under the constraint of fitting *both* signal channels, the only sets of parameters capable of giving acceptable (but not excellent) fits were those shown in Table 1. To enable assessment of the quality of the fits, Fig. 6 shows the best-fitted theoretical curves by trial-and-error to one of the genuine £10 group data sets. Figure 7 shows its counterpart for the counterfeit £10 data set. Best-fits of similar quality were also made to the U.S. banknotes and the results are shown in Table 1. No attempt was made to tabulate the optical parameters obtained from the fittings, either visible or IR, since the laser PTR signal is well-known to depend sensitively on the state

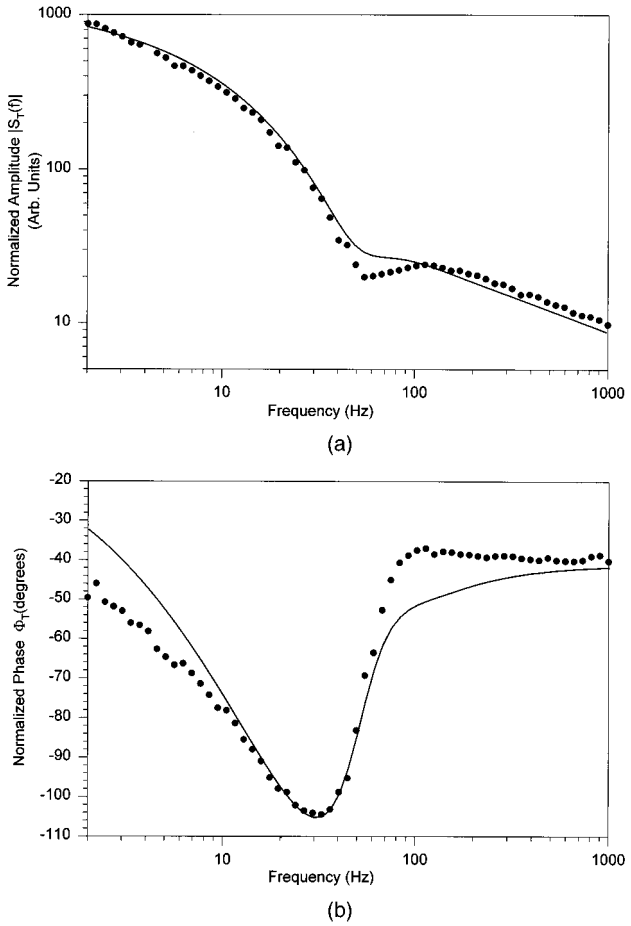

Fig. 7 Similar to Fig. 6 for a high-quality British £10 forgery. For the best-fit thermophysical parameters see Table 1. The optical parameters were $\beta_s = 1.3 \times 10^5$ m^{-1}, $\beta_{IR} = 6.0 \times 10^4$ m^{-1}, and $Q = 0.62$.

of the surface via its infrared emissivity,[3] and thus it is expected that substantial variations may occur in the values of these parameters as functions of the lifetime and past history of the bill. Note, however, that definitive measurements of α_s and, to a lesser extent, k_s may be made as shown in Table 1, despite the aforementioned difficulty with PTR detection of optical properties.

In the fits of Figs. 6 and 7 and for the rest of the data sets, tolerance to parameter variations depended on the particular parameter. The positions of the local minima in the phases and amplitudes, primarily depend most sensitively on the value of thermal diffusivity and less so on that of thermal conductivity. These extrema are physically the results of thermal standing-wave interference in the bulk of the substrate paper of the bill sample and as such they depend strongly on its thickness and the thermal diffusivity.[9] They also depend more weakly on the thermal coupling coefficient b_{gs} at the paper-gas interface[9] through which the value of k_s is obtained [Eq. (8)]. Therefore, varying these thermophysical parameters to match the positions, $f_{\min}$, of the extrema could be done without having to consider changes in the optical properties. Among the latter, the two effective optical absorption/scattering coefficients β_s and β_{IR} controlled the steepness of the curvature around the minima, while β_{IR} alone controlled the absolute height of the phase (trough-to-peak) and amplitude upturn past the minimum. The value of Q impacted the width (broadening) of the extremum lineshape. Therefore, it can be seen from this discussion that the use of two simultaneous fitting data channels (amplitude and phase) can narrow significantly the range of best-fitted values for any one parameter of the multiparameter fit, as optical parameters impact the detailed shape of the curves differently from the thermophysical parameters. For these reasons, our confidence in the values of the thermal diffusivities is the highest, followed by those of β_{IR} and the thermal conductivities. Unfortunately, as already stated, surface conditions greatly affect the values of the optical parameters measured[10] by PTR. Furthermore, it is quite difficult to reposition the pump laser beam *exactly* at the same spot on a given bill, or on consecutively tested bills; this also aggravates the uncertainty of reproducibility of the optical coefficients from one sample to the next. To produce the data in Figs. 2 to 4 and 6 to 7, dark features were chosen as much as possible for laser beam impingement on the bill under examination. For instance, for the £10 bills, we chose to probe in the almost black region of the image of the Queen's hair. This yields a high Q value, which enhances the ''dip'' in the amplitude spectrum and thus helps the more accurate determination of $f_{\min}$, the frequency where the minimum appears.

Based on the preceding, the values of β_s and β_{IR} obtained through fits of the theory to the experimental data have only been considered as characteristics of a *given bill*, which may vary substantially with handling history, age and (perhaps) year of issue of the denomination, although no statistical evaluation of these factors has been performed at this stage.

The quality of the optimum fits in Figs. 6 and 7 varies within a given curve. To obtain the *best overall simultaneous fits* of the theory to the laser PTR amplitude and phase data three compromises had to be made: typically, the low-frequency end of the phase data below 10 Hz and the high-frequency end above 100 Hz could not be fitted well. Furthermore, the actual line shape of the amplitude minimum was usually sharper than the theoretical line shape. The low-frequency discrepancies are likely due to the inadequacy of the reference (steel) sample to reproduce exactly the 1-D transfer function of the instrument: 3-D effects have been observed previously[11] with steel samples below 10 Hz even with laser beam sizes 5 or 10 mm. The currency bills, however, behaved in an entirely 1-D manner in that same frequency region, owing to the very large beam size compared to the sample thickness. The phase discrepancies observed at the high-frequency range of Figs. 6 and 7 are hypothesized to be due to the optical (visible and IR spectral) nonuniformity of the surface absorptance Q across the large beam spot size. This quantity was assumed to be of uniform optical density in the theoretical treatment (Fig. 5), but it was observed to vary laterally substantially, depending on the feature of the image on the bill probed by the laser. The photothermal (linear-scale) phase ''height'' [minimum-to-near flat region in Figs. 6(b) and 7(b)] is expected to be more sensitive than the (logarithmic-scale) amplitude to optical nonuniformities across the front surface of the bill, which affect the actual position of the thermal-wave heat centroid in the bulk of

the substrate paper. Additional theoretical development will be required to assess the importance of these lateral optical nonuniformities on the PTR phase. Intuitively, their presence would tend to have a mixed optical penetration-depth effect on the phase shift as the thermal wavefront moves through the critical frequency f_{crit} from the thermally thin, $\mu_s(f)>L$, to the thermally thick, $\mu_s(f)<L$, condition,[7] where $\mu_s(f_{\text{crit}})=L$ [see Eq. (1)]. The result would thus be expected to affect the phase gradient across the critical frequency regime, where the $f_{\min}$ appears. An analogous effect on the local amplitude minimum would also be anticipated. In Figs. 6 and 7 the best-fit values of Q (0.7 and 0.62, respectively) indicate that the fraction of the incident radiation retained by the surface layer, given by $1-e^{-Q}$, is approximately 0.5, i.e., there was substantial optical penetration of these bills. These almost equal values of Q are testimony to the high quality of the forgery and also to the inadequacy of its detection through purely optical means.

Turning to Table 1, it can be seen that the present laser PTR technique can detect variations in the thermophysical properties even of genuine £10 bills. The percentage changes of the thermal diffusivity (column 3) might be expected to reflect equal changes in the values of the thermal conductivity (column 4), from the definitional linear relationship of these quantities:

$$\alpha_s=\frac{k_s}{C_s\rho_s}, \tag{10}$$

where C_s is the specific heat capacity of the substrate paper and ρ_s is its mass density. The fact that the variations in k_s follow those of α_s only qualitatively, is indicative of either further individual variations in these latter thermophysical parameters, or, most likely, of the lower resolution of the k_s measurement by the present technique, as this parameter enters the theoretical formalism weakly, only through the gas-paper interface boundary conditions. In any case, it is important to notice that the values of *both* α_s and k_s of the counterfeit £10 bill are well outside the standard deviation limits of those of the genuine £10 bills when statistically averaged over the size of the (four) samples. This fact may be significant in future assessments of the current technology as a forensic tool against the proliferation of counterfeit bills.

Finally, there exist large variations between the thermophysical values of the $50 bills. Given that no statistical sampling was performed, it can only be stated that, assuming a spread in the properties of the genuine bills similar to those of the £10 samples, the present technique can easily resolve the presence of the counterfeit. The case of the $100 bill is, however, somewhat more challenging: robust statistical analysis will be required, including the calculation of standard deviations in genuine bills as functions of age and serial printing, to determine statistical fluctuations within samples of genuine bills, and the resolution limits of the technique. This type of analysis is currently under investigation in our laboratory and will be reported in a future publication.

4 Conclusions

Laser-induced IR PTR was applied for the first time to the forensic measurement of the thermophysical transport properties of genuine and counterfeit bills of two major world currencies. Whereas no optical or FTIR signals could be obtained, the PTR technique produced high-quality reproducible frequency scans. A theoretical model of the PTR signal from printed paper[5] was applied to the interpretation of the experimental data. Acceptable-to-good fits were obtained, which were optimized through a trial-and-error procedure.

The best fits yielded the values of thermal diffusivity and thermal conductivity for a British £10 high-quality counterfeit bill, and indicated well-resolved discrepancies beyond the standard deviation of the statistically calculated values from a sample of four genuine £10 bills. Nonstatistical results with U.S. $50 and $100 bills showed very highly resolved genuine-counterfeit differences in thermophysical properties for the former denomination, and substantially closer values for the latter. The results were tabulated in Table 1. The implications of the present work as a noncontact, nonintrusive diagnostic methodology for currency-bill forgeries are broad and novel, since laser PTR measurements of the thermophysical transport properties are primarily functions of the manufacture and texture of the substrate paper on which a currency and denomination is printed, rather than on the details of the print design or dye chemistry. This characteristic of the technique generates the possibility of monitoring the origins and history of the paper on which forgeries are printed, along with its ''user-friendly'' diagnostic power, which can be implemented on-line and does not require specially trained police professionals to discern minute variations in the print design of increasingly more sophisticated forgeries.

Acknowledgements

The authors are indebted to the Criminology Laboratory of the Nicosia Police Headquarters for supplying the counterfeit specimens used in this work, and for useful discussions with M.-E. Eleftheriou and Cyprus Police counterfeit currency expert Officer A. Nicolaides. The collaboration of the Bank of Cyprus in providing genuine British pound and U.S. dollar denominations for comparisons is also gratefully acknowledged.

References

1. R.E. Imhof, B. Zhang and D.J.S. Birch, ''Photothermal radiometry for NDE,'' in *Progress in Photothermal and Photoacoustic Science and Technology, Vol. II*, A. Mandelis, Ed., pp. 186–236, Prentice-Hall, Englewood Cliffs, NJ (1994).
2. A.C. Tam, ''Pulsed laser photoacoustic and photothermal detection,'' in *Photoacoustic and Thermal Wave Phenomena in Semiconductors*, A. Mandelis, Ed., pp. 176–197, North-Holland, New York (1987).
3. R.D. Tom, E.R. O'Hara and D. Benin, ''A generalized model of photothermal radiometry,'' *J. Appl. Phys.* **53**, 5392–5400 (1982).
4. A. Rosencwaig, *Photoacoustics and Photoacoustic Spectroscopy*, Vol. 57, J.D. Wineforder, Series Ed., *Chemical Analysis* (Wiley, New York, 1980).
5. A. Mandelis, M. Nestoros, A. Othonos and C. Christofides, ''Thermophysical characterization of commercial paper by use of laser infrared radiometry,'' *J. Pulp Paper Sci.* (in press).
6. A. Nicolaides, Criminology Laboratory of Police Headquarters, Nicosia, Cyprus, private communication (1996).
7. A. Rosencwaig and A. Gersho, ''Theory of the photoacoustic effect with solids,'' *J. Appl. Phys.* **47**, 64–69 (1976).
8. D. Lide, *CRC Handbook of Chemistry and Physics*, 74th ed., pp. 6-1, 6-199, Chemical Rubber Company (CRC), Cleveland, OH (1993).

9. J. Shen and A. Mandelis, ''Thermal-wave resonator cavity,'' *Rev. Sci. Instrum.* **66**, 4999–5005 (1995).
10. A. Mandelis, K. McAllister, C. Christofides and C. Xenofontos, ''A pilot study in non-contact laser photothermal archaeometry of ancient statuary pedestal stones from Cyprus,'' *Archaeometry* **37**, 257–270 (1995).
11. E. MacCormack, A. Mandelis, M. Munidasa, B. Farahbakhsh and H. Sang, ''Measurements of the thermal diffusivity of aluminum using frequency-scanned, transient-, and rate-window photothermal radiometry. Theory and experiment,'' *Int. J. Thermophys.* (in press).

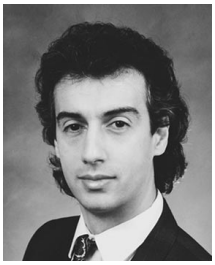

Andreas Othonos received his BSc, Msc and PhD degrees in physics from the University of Toronto in 1984, 1986, and 1990, respectively. His doctoral dissertation research was conducted in the area of carrier and phonon dynamics in semiconductors. Since 1990, he has been a research scientist with the Ontario Laser and Lightwave Research Centre. He has published more than 35 papers in various refereed journals, along with a number of invited chapters in books and invited review papers. His current research interest are ultrafast carrier dynamics in semiconductors, nonlinear optics, fiber optic lasers and fiber Bragg gratings.

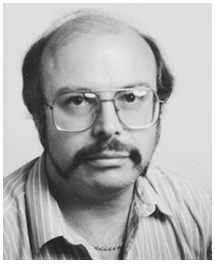

Andreas Mandelis received his BS in physics from Yale University, New Haven, Connecticut, and an MA in applied physics, an MSE in mechanical and aerospace engineering, and a PhD in applied physics from Princeton University, New Jersey. From 1979 to 1981 he was a member of the scientific staff with Bell-Northern Research, Ottawa, Canada, involved in silicon research and development. Since 1981 he has been with the University of Toronto, Canada, where he is currently a professor of mechanical, industrial and electrical engineering and directs the Photothermal and Optoelectronic Diagnostics Laboratory. He has published over 130 research papers in refereed journals, coauthored two books, including *Physics, Chemistry, and Technology of Solid-State Gas Sensor Devices*, holds two patents, and has been the editor-in-chief of the series ''Progress in Photothermal and Photoacoustic Science and Technology.'' His research interests are photothermal instrumentation and measurement science and applications to electronic and manufacturing materials nondestructive evaluation. Dr. Mandelis is fellow of the American Physical Society, and a member of the SPIE, Sigma Xi, and the Optical Society of America.

Marios Nestoros received his BSc in physics from the University of Athens in 1993. He recently completed his MSc requirements and now is working toward his PhD in the Physics Department of the University of Cyprus. His research interests include photothermal characterization of semiconductors and selective coatings, and laser-semiconductor interactions.

Constantinos Christofides received BSci and MSci degrees in physics from Grenoble University, France, and a PhD in 1986 in applied physics from the National Polytechnic of Grenoble. Since 1995 he has been an associate professor in the Department of Natural Sciences at the University of Cyprus, where he was an assistant professor from 1992 to 1995. He was a postdoctoral fellow from 1987 to 1988 at the University of Sherbrooke, Quebec, Canada, and a research associate at the University of Toronto from 1988 to 1992. His research interests are matter-light interaction, photothermal phenomena, laser-semiconductor interactions, optoelectronic sensors, solar materials and applications.